Electronic Supplementary Material (ESI) for Journal of Materials Chemistry A.

Supplemental Information

Impact of Varying Side Chain Structure on Organic Electrochemical Transistor Performance: A Series of Oligoethylene Glycol-substituted Polythiophenes

Shinya E. Chen,[a] Lucas Q. Flagg,[b†] Jonathan W. Onorato,[c†] Lee J. Richter,[b] Jiajie Guo,[a] Christine K. Luscombe,[acde] David S. Ginger[ad*]*

[a] ~ Molecular Engineering and Science Institute, University of Washington, Seattle, WA 98195, United States.

[b] ~ Materials Science and Engineering Division, National Institute of Standards and Technology, Gaithersburg, Maryland 20899, United States.

[c] ~ Department of Materials Science and Engineering, University of Washington, Seattle, WA 98195, United States.

[d] ~ Department of Chemistry, University of Washington, Seattle, WA 98195, United States.

[e] ~ Current Address: pi-Conjugated Polymers Unit, Okinawa Institute of Science and Technology Graduate University, Onna-son, Okinawa, 904-0495, Japan.

[†] These two authors contributed equally to the work.

* Corresponding Author. E-mail christine.luscombe@oist.jp, dginger@uw.edu

TABLE OF CONTENTS:

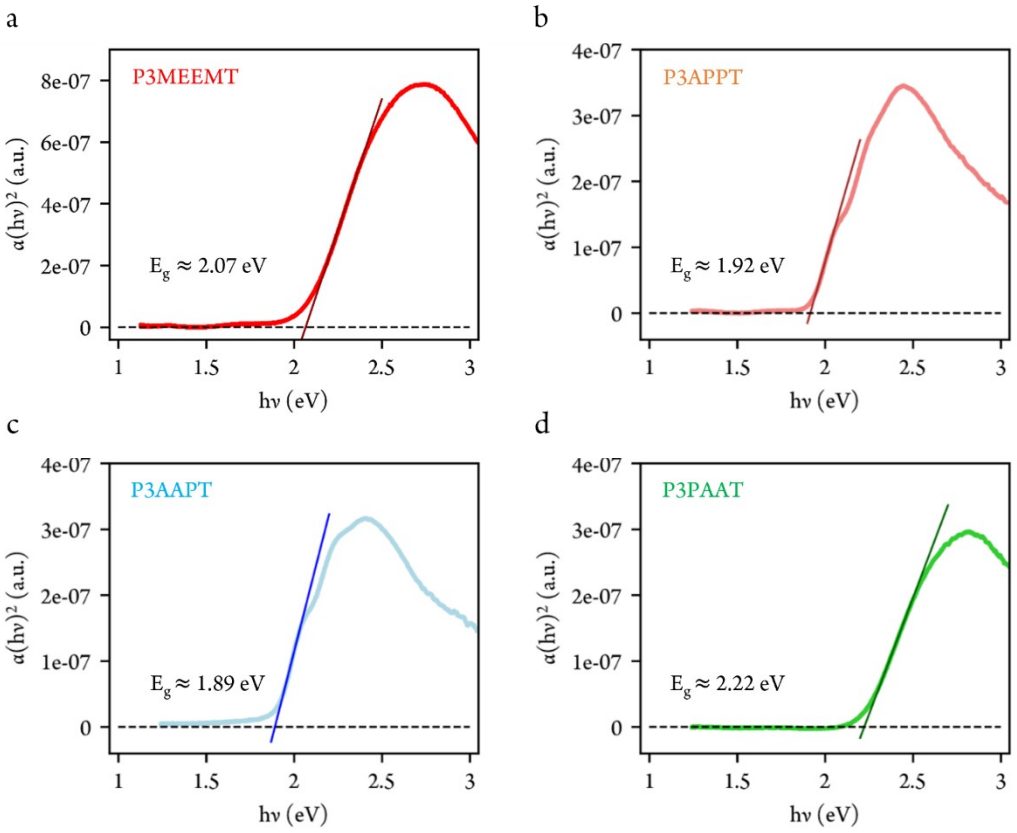

Figure S1. *Determination of optical gap of polymers via Tauc plot.(a) P3MEEMT (b) P3APPT (c) P3AAPT (d) P3PAAT. Dash lines are guide for the eye.*

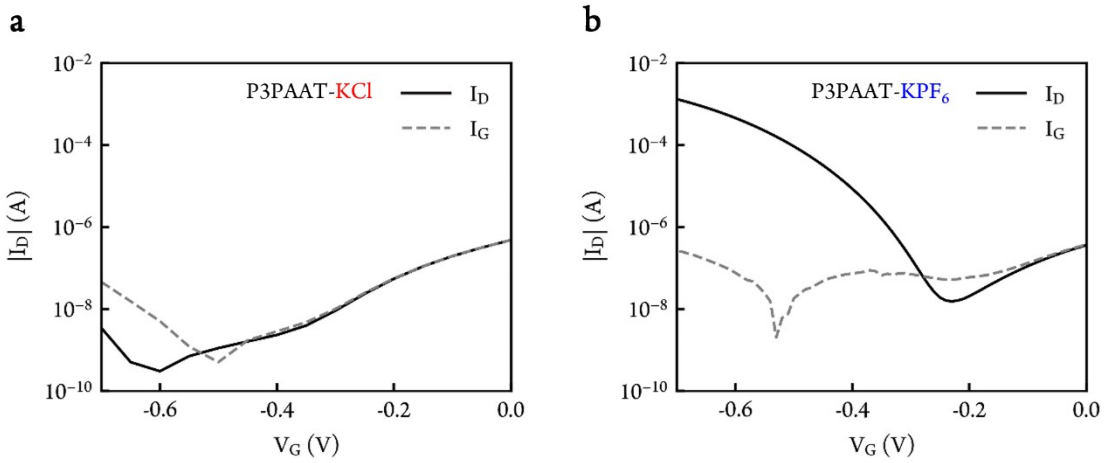

***Figure S2**. Organic electrochemical transistor, OECT, transfer curve of P3PAAT in (a) 100 mmol/L $KCl_{(aq)}$ and (b) 100 mmol/L $KPF_{6(aq)}$. Channel width/length = 4000 µm/10 µm. See main text for notation of polymer structure. Drain voltage, V_D = -0.6 V. Drain current, I_D. Gate voltage, V_G. Gate current, I_G.*

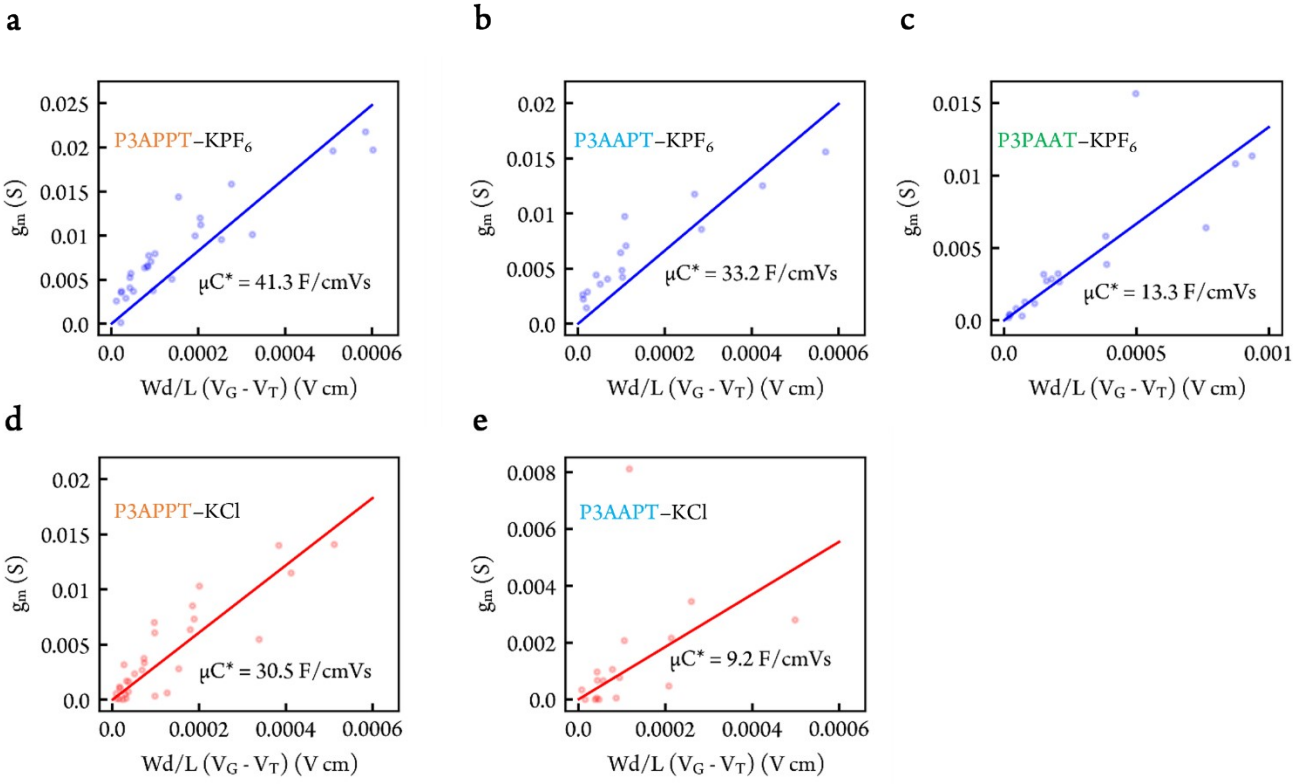

***Figure S3.** Determination of OECT figure of merit μC* (μ carrier mobility and C* volumetric capacitance) of reduced-oxygen-content side chain polymers in 100 mmol/L $KPF_{6(aq)}$ (a) P3APPT (b) P3AAPT (C) P3PAAT and in 100 mmol/L $KCl_{(aq)}$ (d) P3APPT (e) P3AAPT. Each data point represents one transistor device. See main text for notation of polymer structure.*

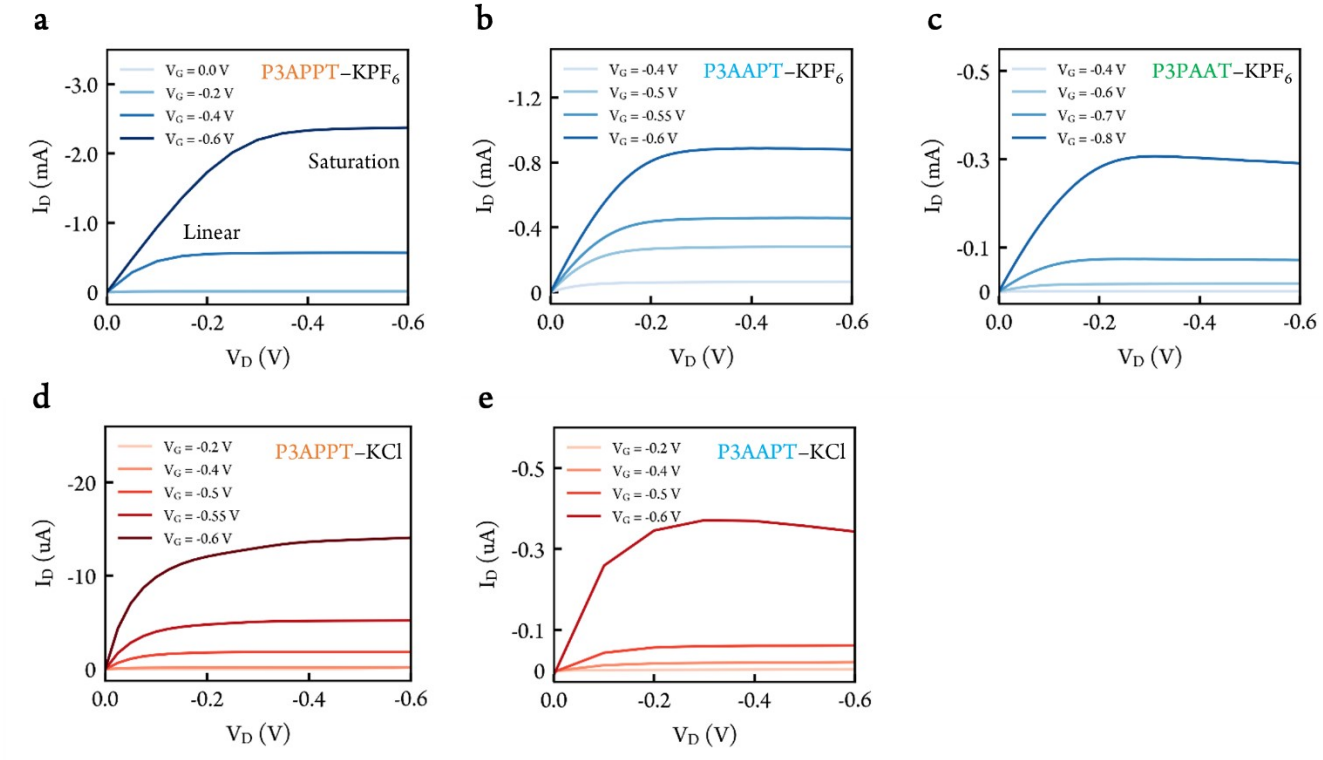

Figure S4. *OECT output curves of reduced-oxygen-content side chain polymers in 100 mmol/L $KPF_{6(aq)}$ of (a) P3APPT (b) P3AAPT (C) P3PAAT and in 100 mmol/L $KCl_{(aq)}$ (d) P3APPT (e) P3AAPT. Channel width/length = 800 µm/10 µm.*

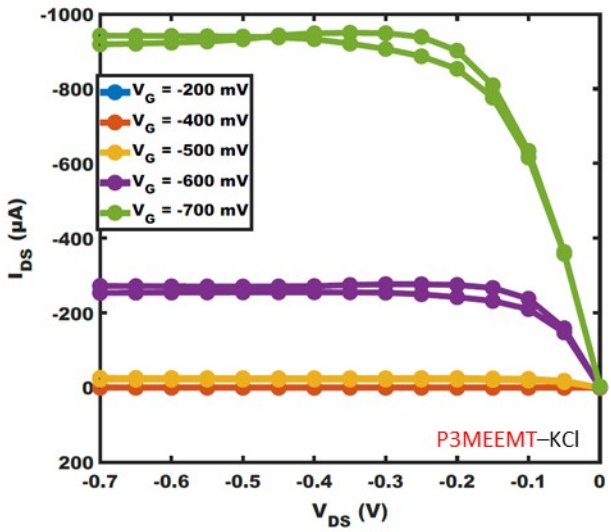

Figure S5. *OECT output curve of poly(3-{[2-(2-methoxyethoxy)ethoxy]methyl}thiophene-2,5-diyl) (P3MEEMT) in 100 mmol/L $KCl_{(aq)}$ obtained from Flagg et al.*[1]

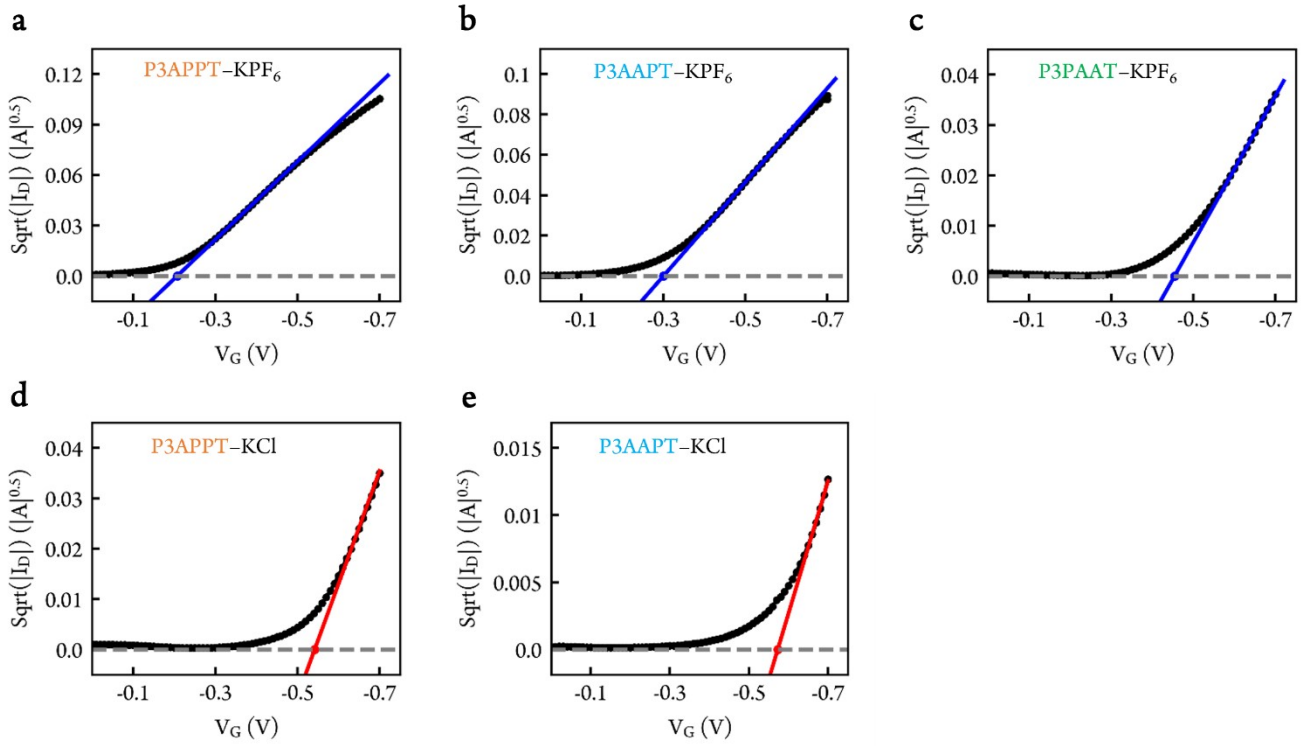

Figure S6. *Determination of threshold voltage (V_T) of reduced-oxygen-content side chain polymers in 100 mmol/L $KPF_{6(aq)}$ (a) P3APPT (b) P3AAPT (C) P3PAAT and in 100 mmol/L $KCl_{(aq)}$ (d) P3APPT (e) P3AAPT. Channel width/length = 4000 µm/10 µm. Grey dash lines are guide for the eye.*

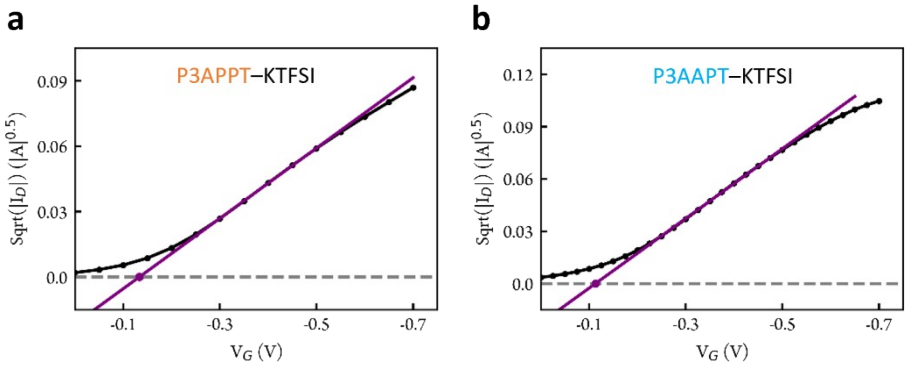

Figure S7. *Determination of V_T of reduced-oxygen-content side chain polymers in 100 mmol/L $KTFSI_{(aq)}$ (a) P3APPT (b) P3AAPT. Channel width/length = 2000 µm/10 µm. Grey dash lines are guide for the eye.*

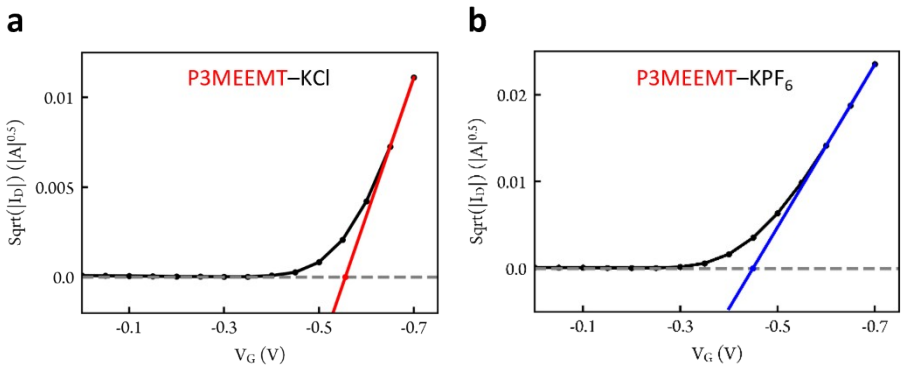

Figure S8. *Determination of V_T of P3MEEMT in (a) 100 mmol/L $KCl_{(aq)}$ and (b) 100 mmol/L KPF_6 obtained from Flagg et al.*[1] *Grey dash lines are guide for the eye.*

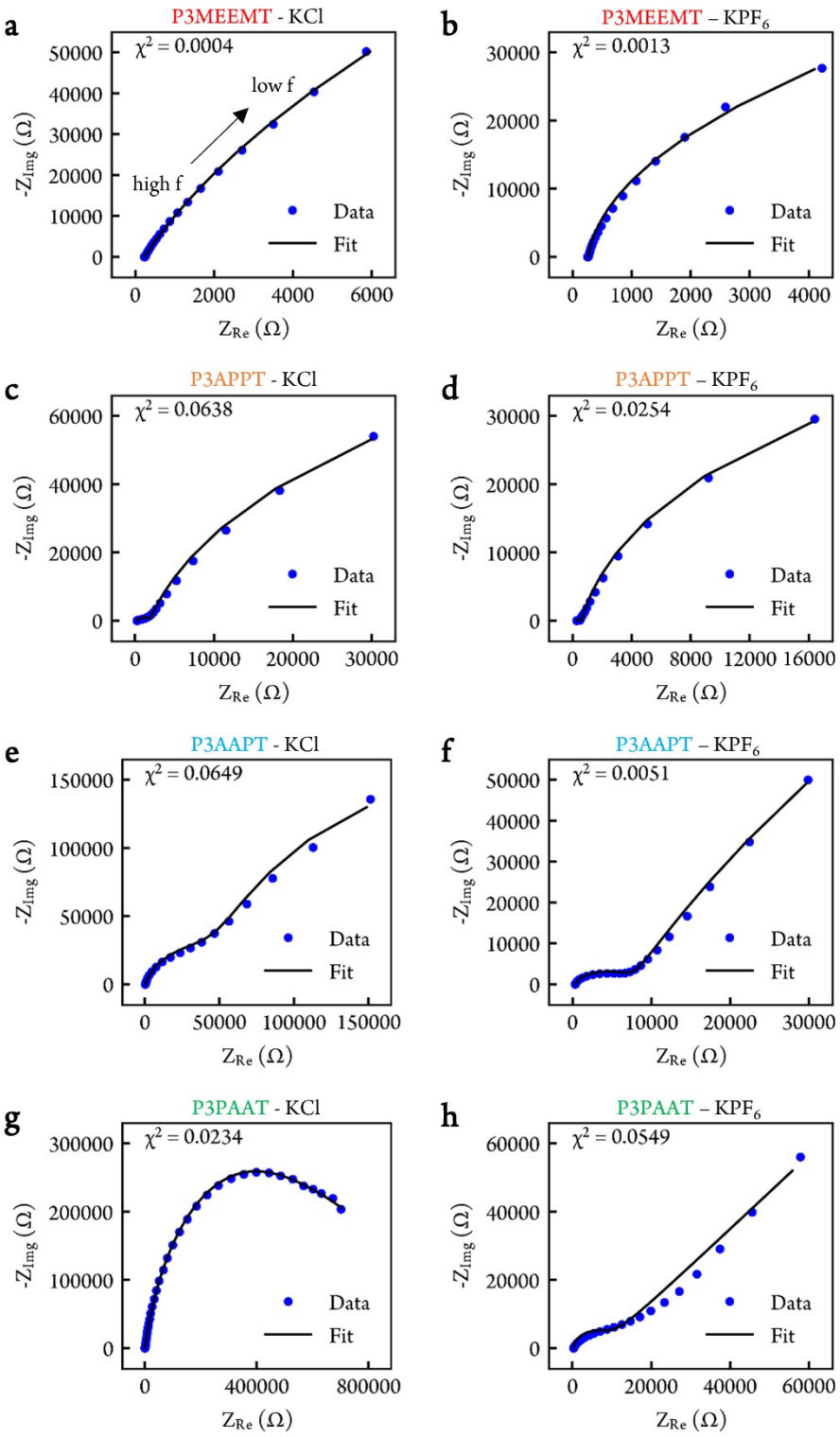

Figure S9. *Example Nyquist plots of (a)(b)P3MEEMT (c)(d) P3APPT (e)(f) P3AAPT (g)(h) P3PAAT in 100 mmol/L $KCl_{(aq)}$ (left) and 100 mmol/L $KPF_{6(aq)}$ (right), respectively.*

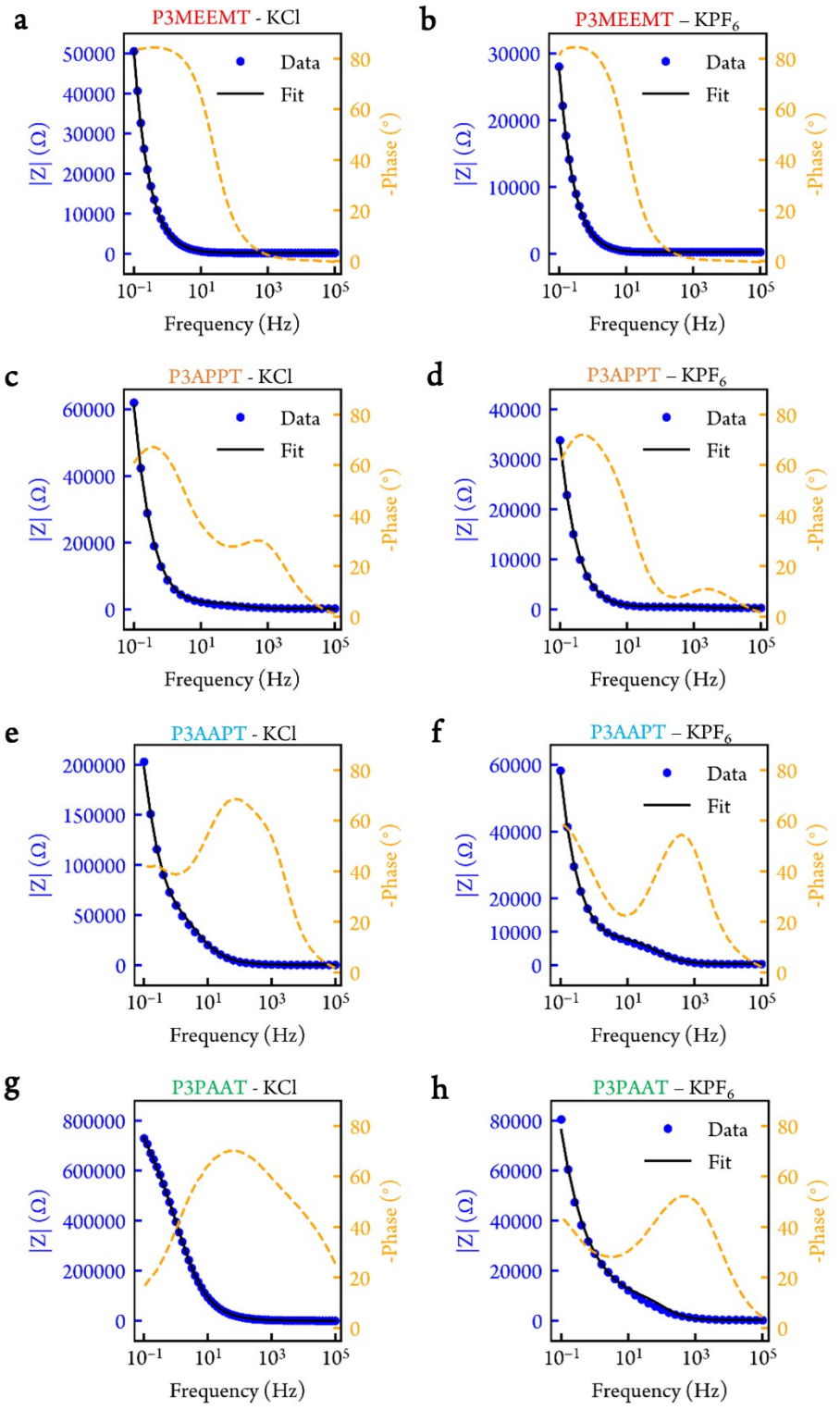

Figure S10. *Example Bode plots of (a)(b)P3MEEMT (c)(d) P3APPT (e)(f) P3AAPT (g)(h) P3PAAT in 100 mmol/L $KCl_{(aq)}$ (left) and 100 mmol/L $KPF_{6(aq)}$ (right), respectively.*

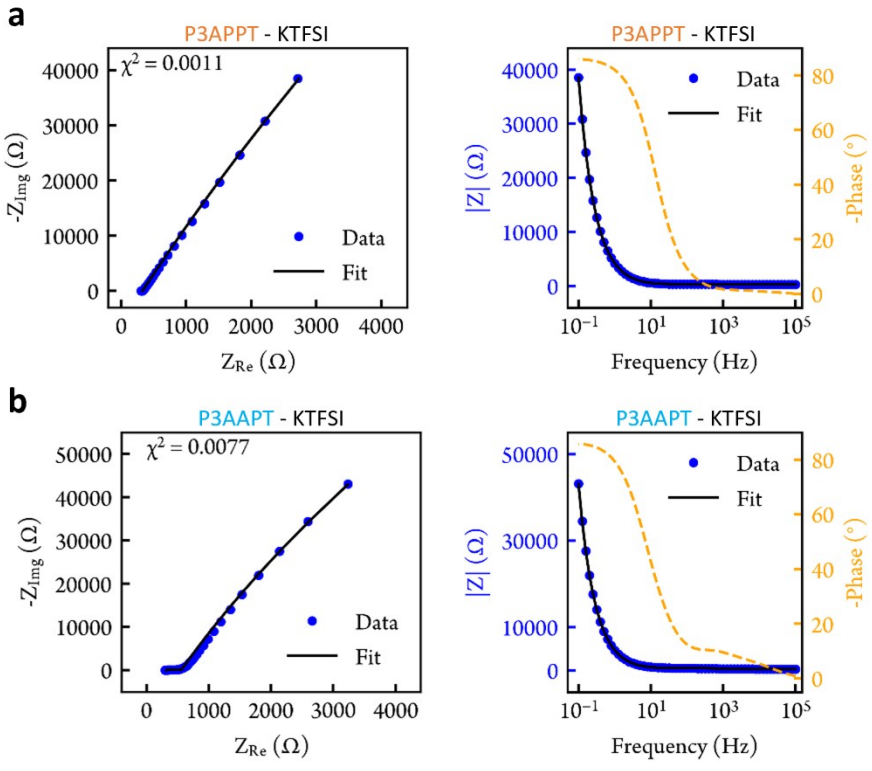

Figure S11. *Example Nyquist plot (left) and Bode plot (right) of (a)P3APPT (b) P3AAPT in 100 mmol/L KTFSI$_{(aq)}$.*

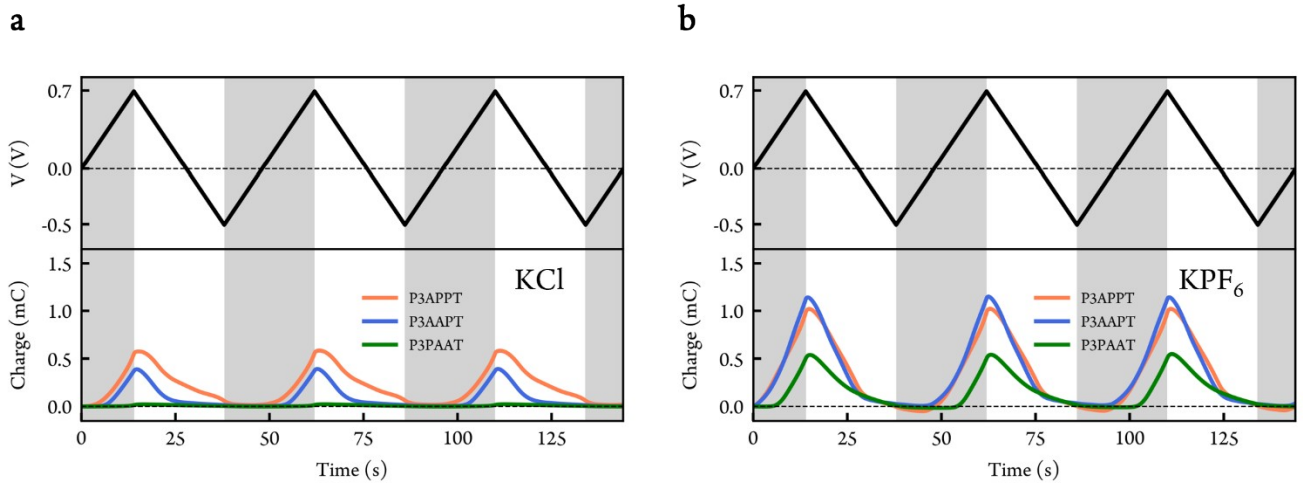

Figure S12. *Charge injection in polymer films during cyclic voltammetry (CV) scans in (a) 100 mmol/L KCl$_{(aq)}$ and (b) 100 mmol/L KPF$_{6(aq)}$. Black dash lines are guide for the eye.*

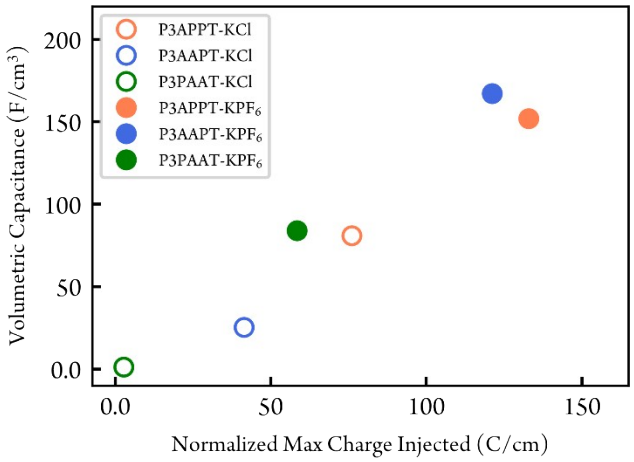

Figure S13. *Volumetric capacitance (via EIS) and charge injected in polymer films (via coulometry). Charge injected in the film was normalized by polymer film thickness*

.

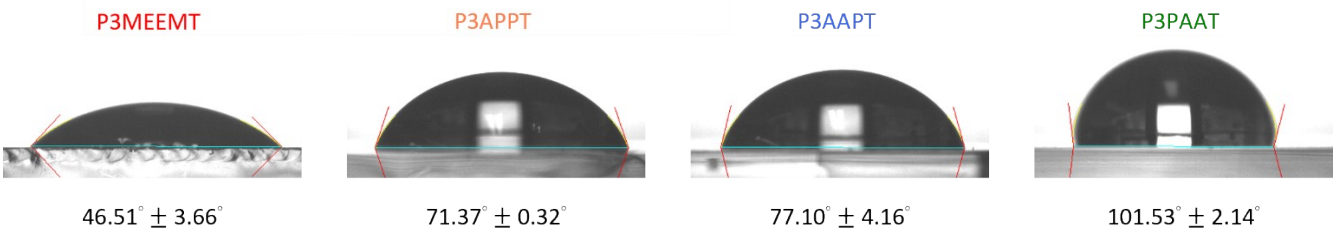

Figure S14. *Water contact angle measurement images. Error bars represent standard error of the mean.*

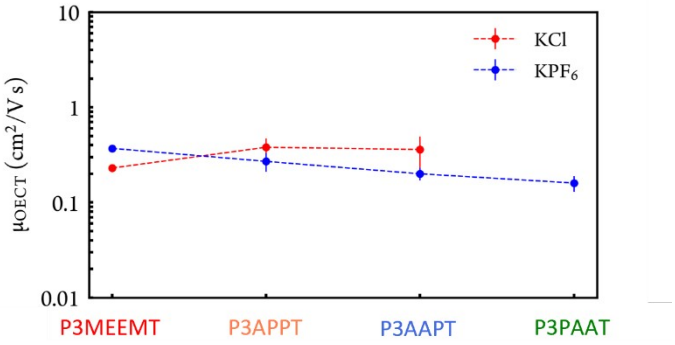

Figure S15. *OECT mobility of polymers in 100 mmol/L $KCl_{(aq)}$ and 100 mmol/L $KPF_{6(aq)}$. Dash lines are guide for the eye. OECT mobility was derived from dividing μC^* by C^* with error propagation. Error bar represents standard error of mean.*

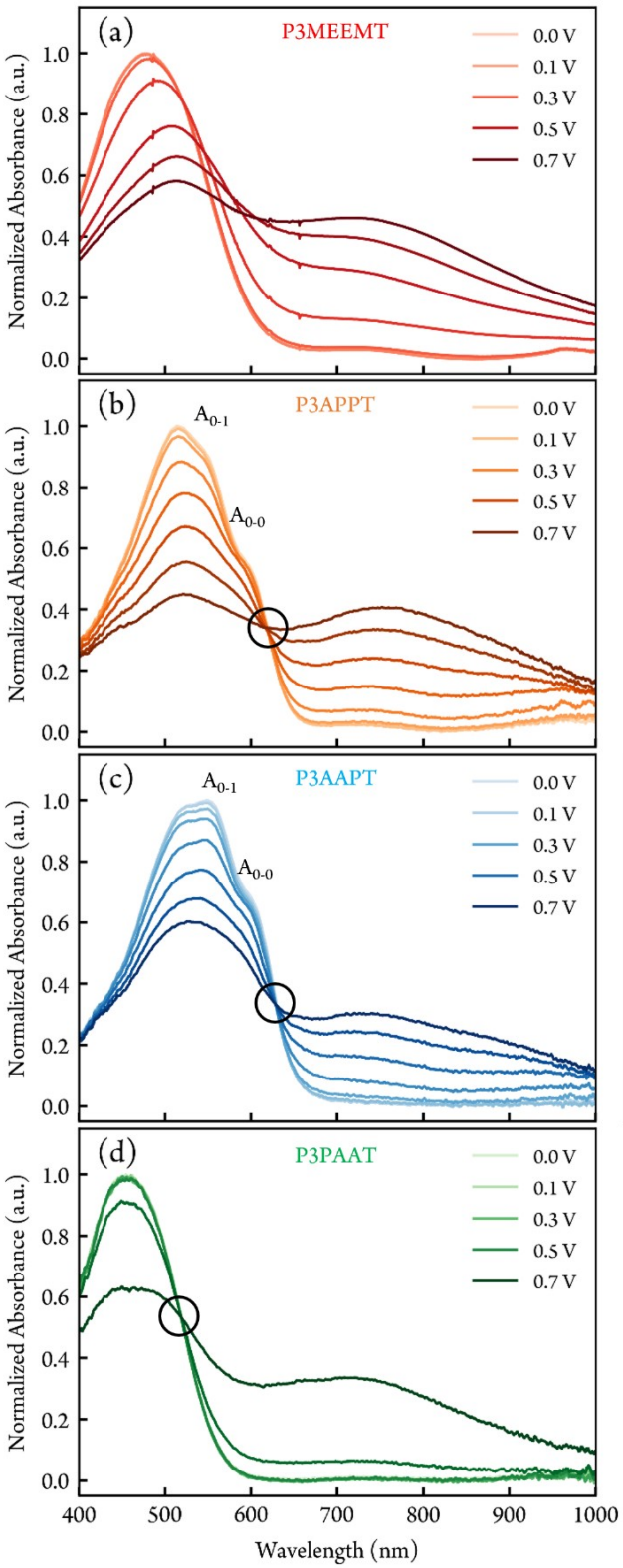

Figure S16. *Spectroelectrochemistry of (a) P3MEEMT (b) P3APPT (c) P3AAPT (d) P3PAAT in 100 mmol/L $KCl_{(aq)}$ electrolyte upon doping. Doping potential = 0.0 V, 0.1 V, 0.2 V, 0.3 V, 0.4 V, 0.5 V, 0.6 V, 0.7 V (vs Ag/AgCl). Black circle indicates the isosbestic point. Only P3APPT and P3AAPT show vibronic progression feature.*

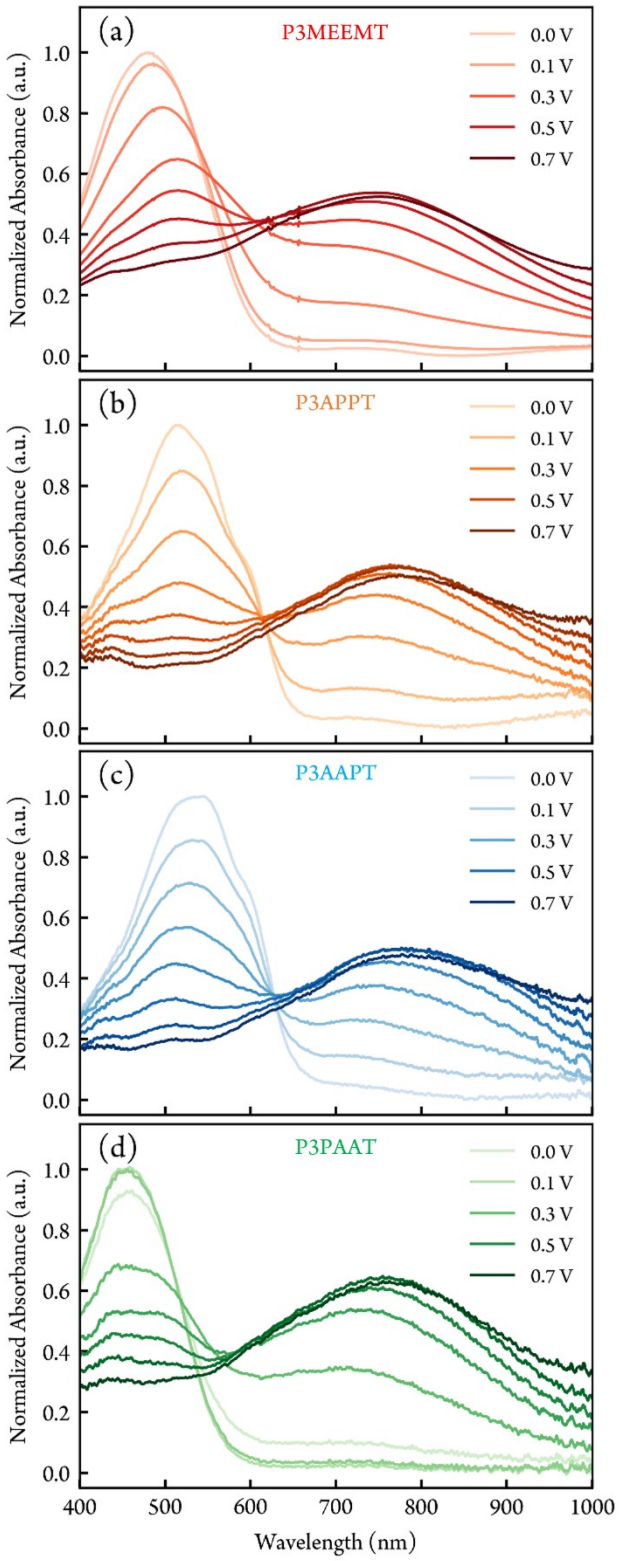

Figure S17. *Spectroelectrochemistry of (a) P3MEEMT (b) P3APPT (c) P3AAPT (d) P3PAAT in 100 mmol/L $KPF_{6(aq)}$ electrolyte upon doping. Doping potential = 0.0 V, 0.1 V, 0.2 V, 0.3 V, 0.4 V, 0.5 V, 0.6 V, 0.7 V (vs Ag/AgCl).*

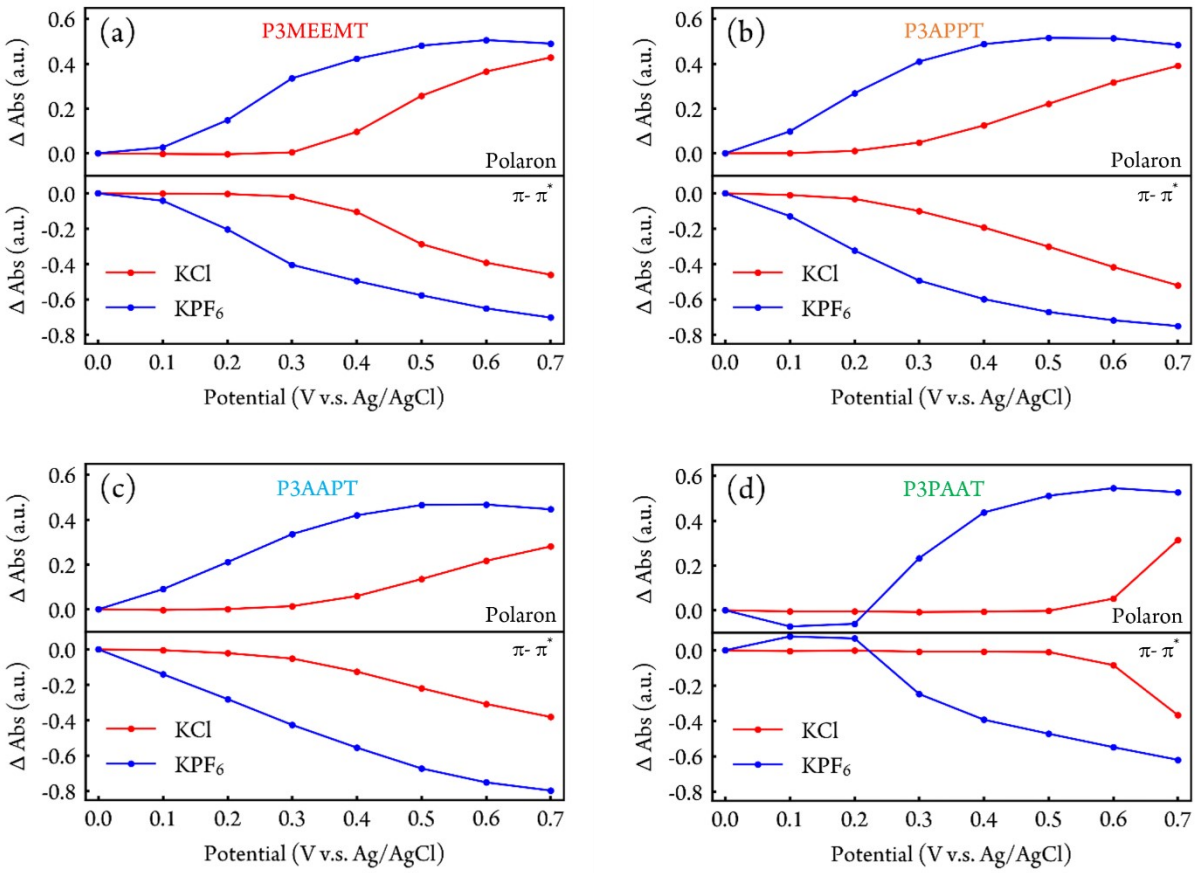

Figure S18. *Comparison of polaron and π-π* peak absorbance change upon doping in 100 mmol/L $KCl_{(aq)}$ and $KPF_{6(aq)}$ (a) P3MEEMT (b) P3APPT (c) P3AAPT and (d) P3PAAT.*

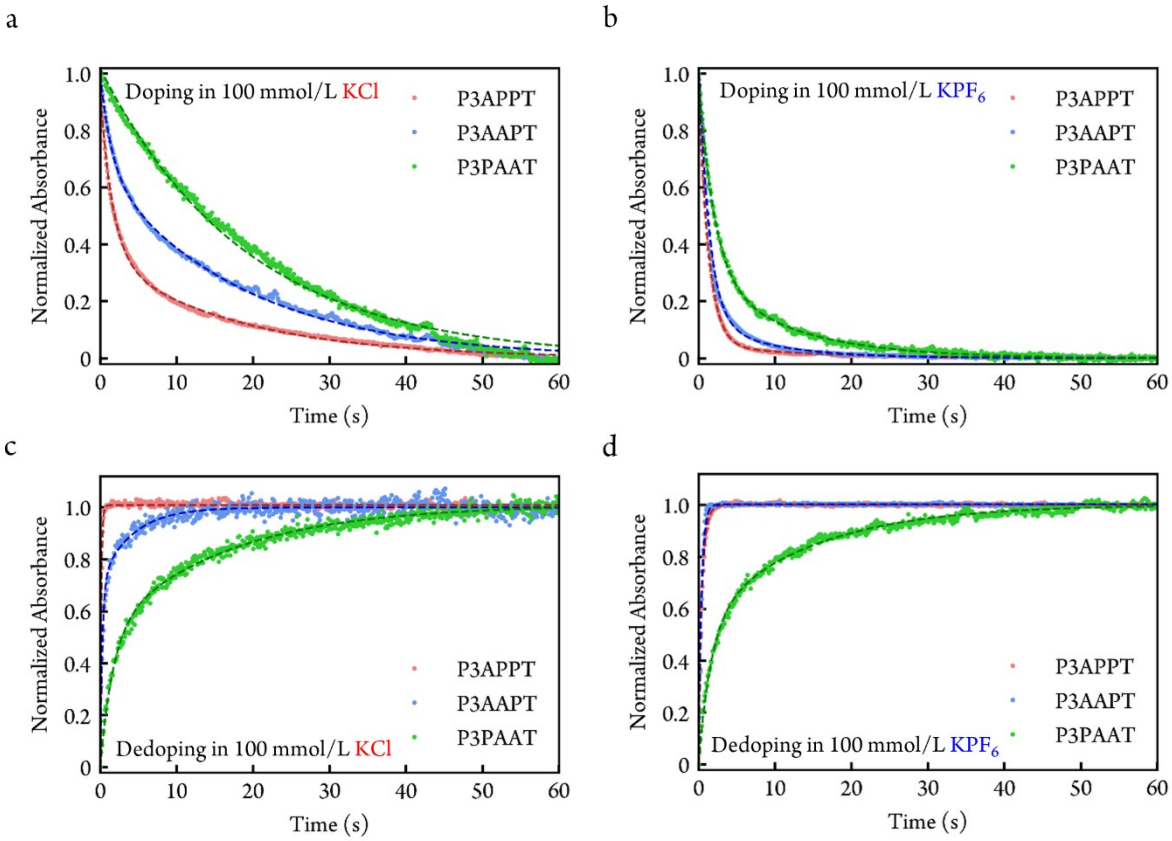

Figure S19. *π-π* peak absorbance change over time during doping in (a) $KCl_{(aq)}$ (b) $KPF_{6(aq)}$ and dedoping in (c) $KCl_{(aq)}$ (d) $KPF_{6(aq)}$. Dash lines represent the fitting results.*

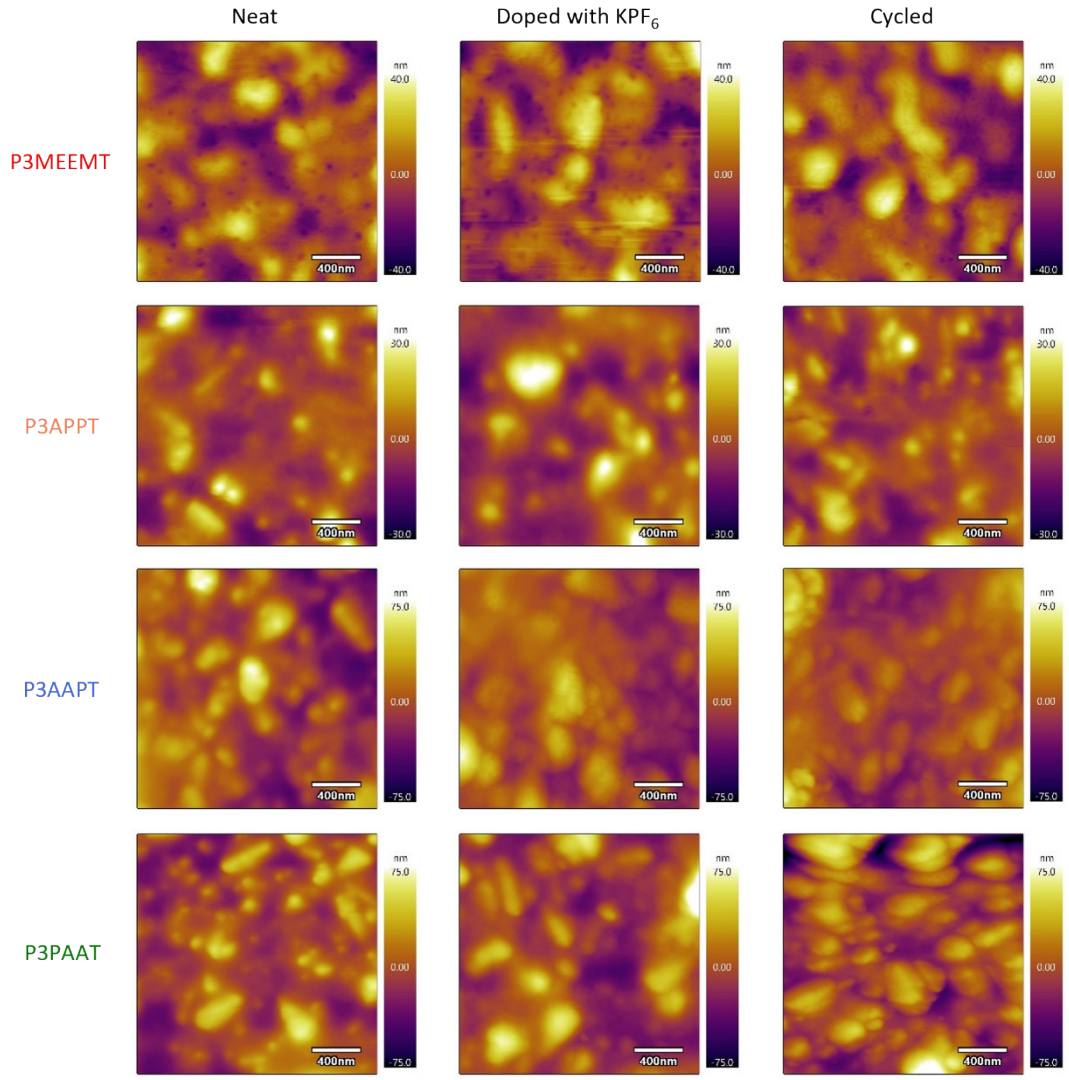

Figure S20. *Atomic force microscopy (AFM) topography images of four polymers in three different states: neat, doped and after three cycles of doping and dedoping. Polymer films were deposited on fluorine-doped tin oxide (FTO) glass substrate.*

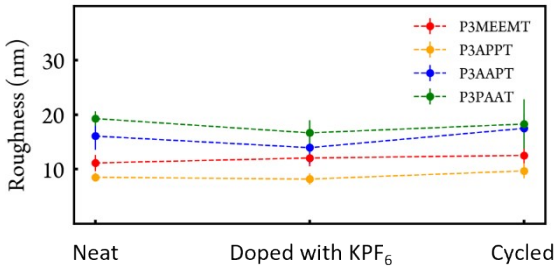

Figure S21. *Roughness of neat polymer films, doped polymer films (with KPF_6), and polymer films doped and dedoped for three cycles with KPF_6. At least four different regions of the film were scanned. Error bars represent standard deviation.*

Table S1. V_T and C^* results of P3APPT and P3AAPT in 100 mmol/L $KTFSI_{(aq)}$

	C^*	V_T
	(F/cm^3)	(V)
P3APPT	143.2 ± 9.4	-0.14 ± 0.01
P3AAPT	107.5 ± 6.5	-0.11 ± 0.02

Table S2. Polythiophene derivatives with isosbestic point observed in spectroelectrochemistry

Polymer	**Electrolyte**	**References**
P3HHT	KCl	2
P3MEET	NaCl	3
PTHS-TMA+-co-P3HT 70:30 mol	NaCl	4
PTHS-TMA+-co-P3HT 51:49 mol	NaCl	4
PTHS-TMA+-co-P3HT 23:77 mol	NaCl	4
P3HT	Polymetric Ionic Liquid	5
P3APPT	KCl	This work
P3AAPT	KCl	This work
P3PAAT	KCl	This work

Conversion of CPE to Capacitor.

Eq S1 shows the impedance form of a constant phase element (CPE). ω is the angular frequency. Y_0 and n are the characteristic parameters of the CPE. A CPE is an imperfect capacitor with n value between 0 and 1. A CPE with n equals to 1 represents an ideal capacitor. Eq S2 shows the impedance form of a capacitor. We applied Eq S3 to convert Y_0 to an equivalent capacitor. ω''_{max} is the frequency where the imaginary part of impedance has its maximum.[6,7]

$$Z_{CPE} = \frac{1}{Y_0 (i\omega)^n} \qquad \text{(Eq S1)}$$

$$Z_C = \frac{1}{C (i\omega)^1} \qquad \text{(Eq S2)}$$

$$C = Y_0 (\omega''_{max})^{n-1}$$ (Eq S3)

References

1 L. Q. Flagg, C. G. Bischak, J. W. Onorato, R. B. Rashid, C. K. Luscombe and D. S. Ginger, *J. Am. Chem. Soc.*, 2019, **141**, 4345–4354.

2 T. Nicolini, J. Surgailis, A. Savva, A. D. Scaccabarozzi, R. Nakar, D. Thuau, G. Wantz, L. J. Richter, O. Dautel, G. Hadziioannou and N. Stingelin, *Adv. Mater.*, 2020, **33**, 2005723.

3 P. Schmode, A. Savva, R. Kahl, D. Ohayon, F. Meichsner, O. Dolynchuk, T. Thurn-Albrecht, S. Inal and M. Thelakkat, *ACS Appl. Mater. Interfaces*, 2020, **12**, 13029–13039.

4 P. Schmode, D. Ohayon, P. M. Reichstein, A. Savva, S. Inal and M. Thelakkat, *Chem. Mater.*, 2019, **31**, 5286–5295.

5 E. M. Thomas, M. A. Brady, H. Nakayama, B. C. Popere, R. A. Segalman and M. L. Chabinyc, *Adv. Funct. Mater.*, 2018, **28**, 1803687.

6 C. H. Hsu and F. Mansfeld, *Corrosion*, 2001, **57**, 747–748.

7 B. Y. Chang, *J. Electrochem. Sci. Technol.*, 2020, **11**, 318–321.